MOLECULAR AND CELLULAR BIOLOGY, July 2004, p. 5978–5988 Vol. 24, No. 13
0270-7306/04/$08.00+0 DOI: 10.1128/MCB.24.13.5978–5988.2004

Characterization of Mice Lacking the Tetraspanin Superfamily Member CD151

Mark D. Wright,[1] Sean M. Geary,[2] Stephen Fitter,[3]† Gregory W. Moseley,[1] Lai-Man Lau,[1] Kuo-Ching Sheng,[1] Vasso Apostolopoulos,[1] Edouard G. Stanley,[3] Denise E. Jackson,[1] and Leonie K. Ashman[2]*

Austin Research Institute[1] and Institute of Reproduction and Development, Monash University,[3] Melbourne, School of Biomedical Sciences, University of Newcastle, and Hunter Medical Research Institute, Newcastle,[2] and Institute of Medical and Veterinary Science, Adelaide,[3] Australia

Received 23 December 2003 /Returned for modification 24 January 2004 /Accepted 28 March 2004

The tetraspanin membrane protein CD151 is a broadly expressed molecule noted for its strong molecular associations with integrins, especially α3β1, α6β1, α7β1, and α6β4. In vitro functional studies have pointed to a role for CD151 in cell-cell adhesion, cell migration, platelet aggregation, and angiogenesis. It has also been implicated in epithelial tumor progression and metastasis. Here we describe the generation and initial characterization of CD151-null mice. The mice are viable, healthy, and fertile and show normal Mendelian inheritance. They have essentially normal blood and bone marrow cell counts and grossly normal tissue morphology, including hemidesmosomes in skin, and expression of α3 and α6 integrins. However, the CD151-null mice do show phenotypes in several different tissue types. An absence of CD151 leads to a minor abnormality in hemostasis, with CD151-null mice showing longer average bleeding times, greater average blood loss, and an increased incidence of rebleeding occurrences. CD151-null keratinocytes migrate poorly in skin explant cultures. Finally, CD151-null T lymphocytes are hyperproliferative in response to in vitro mitogenic stimulation.

The tetraspanin family of membrane proteins consists of at least 26 members in human cells, and many of these proteins are widely expressed in different cell types and tissues. They have a highly conserved overall structure, with four transmembrane passes interconnected by a small and a large disulfide-bonded extracellular loop and their N and C termini located intracellularly. They are represented throughout the phylogeny of multicellular organisms, including schistosomes, *Caenorhabditis elegans, Drosophila melanogaster*, mammals, and plants. Tetraspanins form multimolecular complexes with each other and with other membrane proteins, including integrins, major histocompatibility complex antigens, signaling complexes, and cell-associated growth factors. While their functions are poorly understood at the molecular level, they are clearly involved in cell-cell adhesion, migration, assembly of signaling complexes, and modulation of signal transduction. In particular, they appear to function by regulating the organization and assembly of signaling complexes in membrane microdomains (4, 34, 47; reviewed in references 2, 5, 19, and 54).

Tetraspanins have a role in the pathogenesis of some human diseases. Some are involved in oncogenesis and in the control of metastasis: CD9, CD81, CD82, C0/029, and CD151 can all modulate cancer cell motility both in vitro and in vivo (reviewed in references 5 and 49). Certain tetraspanins have also been identified as receptors or coreceptors for pathogenic microorganisms or toxins. For example, CD81 is a receptor for hepatitis C virus and for malarial parasites (11, 41), and CD9 is a coreceptor for diphtheria toxin (21). Mutations in tetraspanins can also cause human disease; for example, mutations in RDS cause retinal degeneration (50), and mutations in A15 are linked with X-linked mental retardation (57).

The tetraspanin CD151 was initially identified as a marker of human acute myeloid leukemia cells, platelets, and vascular endothelial cells with a monoclonal antibody (1). The cDNA encoding the corresponding antigen was cloned from megakaryoblastic leukemia cells and shown to be a member of the transmembrane 4 or tetraspanin family (10). Isolation of cDNA encoding the same protein from an adult T-cell leukemia line was subsequently reported (18). CD151 is broadly expressed by a variety of cell types, notably epithelial and endothelial cells, muscle cells, Schwann cells, megakaryocytes, and platelets (42). Characteristically, the protein is present on cells juxtaposed with basement membranes and, at least in the case of epithelial cells, it is localized predominantly on the cell surface in contact with this membrane (42). Unlike other tetraspanins that have been studied, CD151 complexes with α6β4 integrin and is a component of hemidesmosomes, which mediate attachment of epithelial cells to the basement membrane (44). CD151 is also localized to cell-cell junctions in endothelial cells (43, 53) and has, together with α3 integrin, recently been shown to be a component of E-cadherin complexes in epithelial cells (6).

Interaction of cells with the basement membrane and with the extracellular matrix in general is mediated by integrins, a

* Corresponding author. Mailing address: School of Biomedical Sciences, University of Newcastle, Callaghan, NSW 2308, Australia. Phone: 61 2 4921 7947. Fax: 61 2 4921 6903. E-mail: leonie.ashman@newcastle.edu.au.

† Present address: Department of Gastroenterology, Flinders University, Adelaide, Australia.

large family of heterodimeric proteins consisting of an α chain and a β chain in various combinations (reviewed in reference 20). Different integrins interact with different extracellular matrixes, although considerable redundancy occurs. The association of CD151 with integrins has been extensively characterized at a biochemical level (6, 9, 23, 40, 43, 44, 53, 55, 56). Based on differential detergent sensitivity, CD151 is considered to form very strong, stoichiometric complexes with α3β1 integrin, moderately strong complexes with α6 and α7 integrins, and less stable, possibly indirect complexes with α2, α4, and α5 integrins and other tetraspanins (2, 19).

CD151 has been reported to be the primary tetraspanin complexing with α3 and α6 integrins, linking them indirectly to other tetraspanins in the tetraspanin web (40). In addition, CD151 is believed to link integrins to the signaling enzymes phosphatidylinositol 4-kinase and protein kinase C (55, 58), to participate in recruitment of a protein-tyrosine phosphatase to cell-cell junctions (6), and to regulate adhesion-dependent activation of Ras (38). Consistent with the role of CD151 as a modulator of integrin function, monoclonal antibodies to the protein block endothelial and epithelial cell migration but have little effect on cell-matrix adhesion under static conditions (9, 43, 53; S. M. Geary, S. Fitter, and L. K. Ashman, unpublished data). To further explore the function of CD151, we generated mice with a homozygous deletion of the corresponding gene.

MATERIALS AND METHODS

Animals. All animal experimentation was carried out with approval from the relevant institutional animal ethics committees.

Generation of CD151-null mice. Construct assembly was initiated by subcloning fragments which spanned CD151 and included adjacent sequences from previously isolated genomic clones (8). Two overlapping clones, pL4C8 and pG8BC1 (Fig. 1A), were isolated and sequenced by primer walking. A *loxP* sequence that also contained an artificial HincII site was introduced into intronic sequences between exons 1c and 2 in clone pL4C8 (Fig. 1B) by overlapping PCR as follows. Two primer sets were designed to amplify across unique restriction sites AflII and BstEII to facilitate introduction of exogenous sequences. The primer pairs were 5′-GACCACTGCTTAAGCTTC and 5′-*ATAACTTCGTATAGCATACATTATACGAAGTTATGTCGAC*AGCTCAGCCAGCTATCTG plus 5′-*GTCGACATAACTTCGTATAATGTATGCTAT*ACGAAGTTATCCAAACTGCAATCATCCG and 5′-CACTGCCATGACAGCCA (complementary sequences are italic). Fragments were amplified with *Pfu* polymerase according to the manufacturer's instructions (Promega, Madison, Wis.) at 95°C for 30 s, 50°C for 45 s, and 72°C for 2 min for 30 cycles. Amplified products from the two separate reactions were purified, mixed, and subjected to a further round of amplification with primers unique to each of the initial PCR products. Amplified products were digested with AflII and BstEII, ligated into pL4C8, and sequenced (pL4C8-HincII/loxp).

Minimal FRT sequences were introduced to facilitate the specific removal of the PGKNeo cassette to allow, if required, the efficient production of conditional knockouts. Introduction of the minimal Flp recombinase target (FRT) sequence 5′ of PGKNeo in the ploxp2PGKNeo construct was performed by overlapping PCR (as described above) with primer pairs 5′-ATTAACCCTCACTAAAGG and 5′-*GAAGTTCCTATACTTTCTAGAGAATAGGAACTTC*AACTCCTCTTCAGACCTA plus 5′-*GAAGTTCCTATTCTCTAGAAAGTATAGGAACTTC*TACGTCCAGCCAAGCTAG and 5′-CCATCTGCACGAGACTAG (complementary sequences are italic). Amplified products were digested with SpeI, ligated into ploxp2PGKNeo, and then sequenced (ploxp2FRTPGKNeo). Introduction of the minimal FRT sequence 3′ of PGKNeo in ploxp2FRTPGKNeo was performed by PCR with *Pfu* (conditions as above) with primer pair 5′-GAGGATCTCGTCGTGAC and 5′-CCCGGGGAAGTTCCTATACTTTCTAGAGAATAGGAACTTCTTCGAGGGACCTAATAAC. Amplified products were digested with NcoI, ligated into ploxp2FRTPGKNeo (digested with XhoI, end filled with Klenow as per standard protocols, and NcoI digested), and then sequenced (ploxp2FRT2PGKNeo). The *loxP*- and FRT-flanked PGKNeo cassette was liberated from ploxp2FRT2PGKNeo with SmaI and then ligated into ScaI-digested

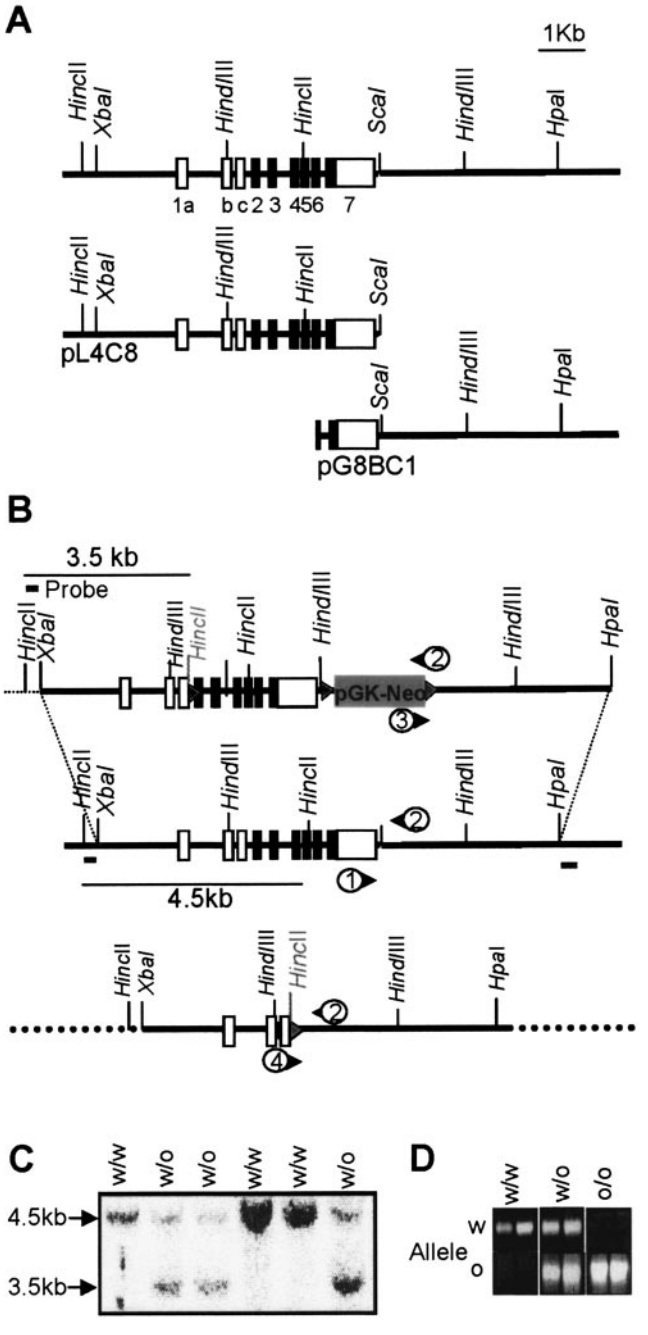

FIG. 1. Targeting the *CD151* gene. (A) CD151 gene structure and overlapping genomic clones pL4C8 and pG8BC1. (B) Targeting strategy. Restriction maps are shown for the targeting vector (top), the wild-type CD151 locus (middle), and the mutated CD151 locus after Cre-mediated recombination (bottom). Coding exons are illustrated as shaded boxes, and noncoding exons are shown as open boxes. *loxP* sites are indicated by triangles. (C) Southern blotting of mouse tail DNA. Germ line transmission was demonstrated by genotyping six littermates derived from a chimeric mouse derived from a CD151-targeted ES cell mated with a C57BL/6 mouse. A probe derived from a HincII/XbaI digest (B) detected a 4.5-kb wild-type and 3.5-kb mutant fragment in HincII-restricted DNA. (D) PCR analysis of mouse tail DNA. The approximate positions of sequence homologous to oligonucleotide primers (indicated by circled numbers in panel B) are shown.

pG8BC (pG8BC_PGKNeo). The backbone of the construct was then prepared by subcloning the XbaI-BamHI fragment from pL4C8-HincII/loxp into pBluescript (KS+) (Stratagene, La Jolla, Calif.). This construct was then digested with BamHI and EcoRV, ligated to the BamHI-HpaI fragment from pG8BC_PGKNeo, and sequenced (pCd151_KO1).

After linearization with XbaI and HpaI, 25 μg of target vector was electroporated into C57BL/6 embryonic stem (ES) cells (26). Transfectants were selected with G418, and genomic DNA from resistant transfectant clones was isolated by standard techniques. Homologous recombinants were identified by Southern blotting. Briefly, a 364-bp 5′ probe, isolated by HincII and XbaI digestion of a segment of the CD151 gene upstream of the targeting vector, was used to probe genomic DNA restricted with HincII. The wild-type fragment was 4.5 kb, and the mutant fragment, created by the introduction of the artificial HincII site (see above), was 3.5 kb (Fig. 1C). Similarly, targeting at the 3′ end of the gene was analyzed with a 752-bp probe isolated by digestion of an HpaI/NcoI fragment located downstream of the final exon 7. Here, genomic DNA was restricted with BamHI, and the wild-type band was 7 kb, whereas successful integration of the pGKNeo cassette resulted in a larger 9-kb fragment.

Chimeras were generated from targeted ES cells with standard methods and crossed with C57BL/6 mice to obtain germ line transmission. Mice that were heterozygous for a correctly targeted mutant CD151 allele were crossed with C57BL/6 Cre recombinase transgenic "deleter" mice to ubiquitously excise the *loxP*-flanked exons 2 to 7 of the CD151 gene in all cells, including germ cells (39).

Deletion and subsequent genotype analysis were performed by PCR with the strategy shown in Fig. 1B. A common reverse primer (designated 2 in Fig. 1B) is homologous to sequence present downstream of exon 7 and has the sequence 5′-CAGCTTAGGACCTCTTCTCA. This primer was used in conjunction with three different forward primers designed to distinguish wild-type, targeted (floxed), and deleted alleles (see Fig. 1B). The forward primers were primer 1 (5′-GCTCCATGTTCCTGTACACT), homologous to sequence in exon 7 and used to detect wild-type alleles; primer 3 (5′-GCCTCTGTTCCACATACACT), homologous to sequence in the neomycin cassette and used to detect targeted (floxed) alleles; and primer 4 (5′-ATGATAACCCACCATGTGTC), homologous to sequence in exon 1b and used to detect deleted alleles. Products were approximately 400 bp in length and amplified with HotstarTaq (Qiagen, Hilden, Germany) with one cycle of 94°C for 15 min, 55°C for 1 min, and 72°C for 30 s, followed by 35 cycles of 94°C for 1 min, 55°C for 1 min, and 72°C for 1 min.

RNA analysis. RNA was isolated from mouse lungs with the RNAshredder kit (Qiagen). Northern blot analyses were performed with standard techniques. Briefly, 15 μg of total RNA was electrophoresed in denaturing gels and transferred by capillary action to Zeta Probe filters (Bio-Rad, Hercules, Calif.). Filters were then probed with ^{32}P-labeled CD151 cDNA (products amplified by primers complementary to the 5′ and 3′ ends of the CD151 ORF: 5′-ATGGGTGAATTCAATGAGAA and 5′-TCAGTAGTGTTCCAGCTTGA). After exposure to a Storm 480 phosphoimager (Molecular Dynamics, Kew East, Victoria, Australia), filters were stripped and reprobed with a glyceraldehhyde-3-phosphate dehydrogenase cDNA probe (amplified by primers 5′-ACAGCCGCATCTTCTTGTGCAG and 5′-CCTAGGCCCCTCCTGTTATTATG).

cDNA was generated from lung RNA with a Moloney murine leukemia virus reverse transcriptase H-point mutant (Promega, Annandale, New South Wales, Australia) by the manufacturer's protocol. cDNA was analyzed for CD151 with the primers specific for the 5′ and 3′ of the CD151 open reading frame (ORF) (see above) or for β-actin with primers GTGGGCCGCTCTAGGCACCAA and CTCTTTGATGTCACGCACGATTTC. The PCR was one cycle of 94°C for 15 min, 55°C for 1 min, and 72°C for 1 min, followed by 30 cycles of 94°C for 1 min, 55°C for 1 min, and 72°C for 1 min.

Peripheral blood and bone marrow analysis. Age- and sex-matched wild-type and CD151$^{-/-}$ mice were anesthetized with halothane applied continuously with an anesthetic machine with flow rates of 3 liters of oxygen/min during anesthesia and 5% halothane delivered into an anesthetic box. Whole blood was collected from the ventricle of mice by cardiac puncture with a 26-gauge needle. Blood (≈700 μl) was withdrawn into a 1-ml syringe and transferred into 0.5-ml tubes containing dipotassium EDTA. These anticoagulated samples were analyzed for red blood cells, white blood cells, and platelet parameters by IDEXX Laboratories (Glenside, Australia) and used to prepare blood films by placing a drop of blood onto a glass microscope slide and thinly spreading it over the glass surface. Films were air-dried, fixed in methanol, and stained with Wright's Romanovsky stain. Bone marrow cells were extracted from the femurs by aspiration with 0.85% (wt/vol) normal saline. Bone marrow films were prepared and fixed as above and stained with May-Grunwald Giemsa Romanovsky stain. Differential counts were performed manually, with analysis of 500 cells per specimen.

Histology and immunohistochemistry. Two-to three-day-old C57BL/6 wild-type and CD151-null mice were euthanized by decapitation, and the skin was removed from the ventral surface. For light microscopy, specimens were fixed in 4% formaldehyde in phosphate-buffered saline (PBS) and paraffin embedded, and 5-μm sections were cut, dewaxed, and stained with hematoxylin and eosin by standard procedures.

For electron microscopy, specimens were fixed in 2.5% glutaraldehyde, and processed for Epon embedding by standard methods; 50- to 60-nm sections were viewed at 80 kV in a Jeol 1010 transmission electron microscope at the Centre for Microscopy and Microanalysis at the University of Queensland, Brisbane, Australia. Images were captured digitally. For immunochemistry, 6- to 8-week-old C57BL/6 and CD151-null mice were euthanized and perfused with 4% (wt/vol) paraformaldehyde in PBS to preserve morphology and remove red blood cells. Kidneys were surgically removed, decapsulated, halved, placed in 30% sucrose solution overnight at 4°C, embedded in OCT compound (Tissue-Tek, Torrance, Calif.), and frozen in liquid nitrogen-cooled isopentane; 5-μm cryostat sections were placed on microscope slides coated with 3-aminopropyltriethoxysilane (Sigma Chemical Co, St. Louis, Mo.).

Sections were fixed in ice-cold methanol-acetone-formalin (47.5:47.5:5, vol/vol) for 45 s, washed, and incubated with 0.3% (vol/vol) H_2O_2 in PBS for 20 min at room temperature to block endogenous peroxidase. Sections were washed and treated with an endogenous avidin-biotin blocking reagent (Zymed, South San Francisco, Calif.) and further blocked with 1% bovine serum albumin (wt/vol) in PBS for 1 h at room temperature. Sections were incubated overnight at 4°C with 5 μg of purified primary antibody (unless otherwise indicated) per ml in PBS–0.1% bovine serum albumin–0.1% NaN_3 containing 10% (vol/vol) heat-inactivated normal equine serum.

The primary antibodies used were polyclonal rabbit antibody to mouse-human α3 integrin, kindly provided by Fedor Berditchevski (University of Birmingham) and monoclonal rat anti-mouse α6 integrin (clone GoH3; Immunotech, Marseille, France). Negative control antibodies were rat immunoglobulin G (Sigma) and normal rabbit serum (Invitrogen, Mulgrave, Australia). Following incubation with primary antibody, sections were washed and incubated for 1 h at room temperature with a 1:500 dilution of biotinylated anti-rabbit or anti-rat immunoglobulin antibody (Chemicon, Temecula, Calif.) in PBS containing 10% (vol/vol) equine serum. Sections were washed and incubated for 30 min at room temperature with a 1:500 dilution of streptavidin-horseradish peroxidase (Chemicon). After washing, sections were incubated for 15 min at room temperature with a freshly prepared and filtered (0.45 μm) solution containing 1.25 mM 3,3′-diaminobenzidine tetrahydrochloride (Sigma) and 0.1% (vol/vol) H_2O_2 in Tris buffer. The reaction was stopped with 0.1% NaN_3 solution, and sections were counterstained with Lillie-Mayer hematoxylin (Australian Biostain, Victoria, Australia).

Keratinocyte isolation and immunofluorescence. Two- to 3-day-old C57BL/6 wild-type and CD151-null mice were decapitated, and the skin was surgically removed and sterilized by sequential washes in sterile PBS (plus penicillin G at 50 U/ml, streptomycin sulfate at 50 μg/ml, and amphotericin B at 0.25 μg/ml), Milli Q water, 70% ethanol, and PBS (plus antibiotics) as described before (17). For isolation of keratinocytes, the skin was incubated overnight at 4°C with dispase (4 mg/ml in PBS). The epidermal layer was peeled off, and the cells were dispersed by vigorous pipetting with trypsin-EDTA for 5 min. The cell suspension was treated with soybean trypsin inhibitor, washed, and cryopreserved until required. Antigen expression was examined by indirect immunofluorescence and flow cytometry as previously described (9). The antibodies used were described above plus rat monoclonal antibodies to murine β1 integrin (clone 9EG7), α4 integrin (clone 346-11A), CD9 (clone KMC8), all from BD Pharmingen, San Diego, Calif., and hamster antibody to murine CD81 (EAT2), kindly provided by Scott Todd, Kansas State University. Bound primary antibodies were detected by biotinylated second-stage antibodies, followed by streptavidin-fluorescein isothiocyanate (FITC).

Skin explant cultures. Punch biopsies were prepared aseptically from neonatal skin (isolated as above) and cultured as described by Mazzalupo et al. (33). After removal of excess fat, explants were generated with a 4-mm cutaneous punch and allowed to adhere to 18-mm coverslips in 12-well tissue culture trays for 5 to 10 min prior to the addition of 1 ml of explant medium (1:1 Dulbecco's modified Eagle's medium-F12 medium, pH 7.2) supplemented with fetal calf serum (10% vol/vol), cholera toxin (0.1 nM), human epidermal growth factor (10 ng/ml), T3 (2 nM), transferrin (5 μg/ml), insulin (5 μg/ml), hydrocortisone (0.4 μg/ml), penicillin G (50 U/ml), streptomycin sulfate (50 μg/ml), gentamicin (32 μg/ml), amphotericin B (0.25 μg/ml), and L-glutamine (0.2 mM). Explant cultures were set up in quadruplicate and maintained at 37°C and 5% CO_2 for up to 6 days, with medium changes every 2 days. Where indicated, after 20 h (before outgrowth became evident), some cultures were treated with mitomycin C (Sigma), 10 μg/ml, for 2 h to block cell proliferation. Explants were washed twice and cultured with explant medium as above. Outgrowth was quantitated by measure-

ment with an eyepiece graticule at eight positions around the circumference of each explant. The average width of outgrowth was calculated for each replicate explant. Photographs were taken with a digital camera (Olympus Camedia C-4040 zoom) attached to an inverted microscope (Olympus model CK40).

Tail bleeding assay of hemostasis. Six- to eight-week-old wild-type and CD151$^{-/-}$ mice were anesthetized with halothane applied continuously with an anesthetic machine with flow rates of 3 liters of oxygen/min and 1.5% halothane delivered via a mask placed over the nose of the mouse; a 2-mm diameter of tail tip was selected with a template, and this portion of the tail was excised with a sharp scalpel blade. The time taken for the flow of blood to cease was recorded. The drops of blood were collected into an Eppendorf tube containing 100 μl of 3.8% (wt/vol) trisodium citrate or collected onto filter paper. The volume of blood lost during the tail bleeding time was quantitated from the drops of collected blood. If bleeding restarted within 1 min, this result was recorded as a rebleed.

Splenocyte and T-cell proliferation. Splenocyte preparations were made in RPMI 1640 medium (Gibco BRL, Grand Island, N.Y.) with 10% (vol/vol) fetal calf serum and 0.1 m[/mu] 2-mercaptoethanol (complete RPMI) with 100-μm cell strainers (Becton Dickinson, Franklin Lakes, N.J.). Erythrocytes were lysed with ACK lysis buffer (0.15 M NH_4Cl, 1 mM $KHCO_3$, 0.1 mM disodium EDTA, pH 7.2). Splenocytes (10^5 cells/well) were stimulated with 1 to 5 μg of concanavalin A (Sigma) or 1 μg of lipopolysaccharide (Sigma) per ml in 96-well plates for various times. Splenic T cells were purified by being passaged twice over a nylon wool column. CD4$^+$ or CD8$^+$ T cells were purified from either the spleen or lymph node by antibody-bead depletion with monoclonal antibody against surface molecules CD11b, GR-1, B220, TER119, and major histocompatibility complex class II, and monoclonal antibody against either CD8α or CD4.

Two rounds of magnetic bead depletion were performed with goat anti-rat immunoglobulin-coated beads (Paesel & Lorei GMBH, Frankfurt, Germany). Purified T cells (2×10^4 cells/well) were stimulated with KT31.1 (anti-CD3) (coated at 10 μg/ml) with or without anti-CD28 (1 μg/ml in solution) in complete RPMI. T cells were pulsed overnight with 1 μCi of [^{3}H]thymidine (Amersham, Little Chalfont, Buckinghamshire, United Kingdom), and incorporation was measured with a scintillation counter (Top Count; Packard, Meriden, Conn.). Data are expressed as mean counts per minute ± standard error of the mean.

Immunization experiments and immunoglobulin detection. Groups of eight mice, both wild-type and CD151$^{-/-}$, were injected intraperitoneally with 100 μg of NP ([4-hydroxy-3-nitrophenyl]acetyl) coupled to keyhole limpet hemocyanin (KLH) (NP_{18}-keyhole limpet hemocyanin conjugation ratio, 18:1) precipitated in alum. Mice were bled, and sera were collected at days 7, 14, and 21 postimmunization. NP-specific antibodies were measured by enzyme-linked immunosorbent assay with 96-well plates (Dynex) coated with 20 μg of NP_{17}-bovine serum albumin. Serially diluted serum samples were applied to the washed plates and incubated for at least 4 h. Horseradish peroxidase-labeled anti-mouse immunoglobulin G1 and immunoglobulin G2a (Southern Biotechnology Associates, Birmingham, Ala.), at a concentration of 1:1,000, were applied for 2 h before washing and signal detection with azinobis(3-ethylbenzthiazolinesulfonic acid) diammonium salt substrate (Sigma). NP-specific monoclonal immunoglobulin G1 was used to generate a standard curve from which relative units were derived. Data are expressed as means ± the standard error of the mean.

RESULTS

Generation of CD151-null mice. To study the function of CD151 in vivo, a CD151-deficient mouse was produced. Maps of the structure of the CD151 gene, the targeting construct, and the targeted and the deleted alleles are shown in Fig. 1A and B. Briefly, the targeting strategy was to introduce a *loxP* site into the intron between exon 1c and the first coding exon (exon 2) and a *loxP*-flanked neomycin cassette downstream of the final coding exon (exon 7). Thus, Cre-mediated recombination would result in the excision of all six coding exons of the CD151 gene. ES cells that had undergone homologous recombination were identified by Southern blotting with probes external to the targeting construct at both the 5′ and 3′ ends (data not shown). Mice carrying successfully targeted (floxed) CD151 alleles were generated from ES cell-derived chimeras by standard techniques and identified initially by Southern blotting (Fig. 1C). Mice carrying CD151-null alleles were generated by crossing floxed heterozygote mice to deleter mice (39) to ensure ubiquitous deletion of *loxP*-flanked sequences. These alleles were identified by PCR analyses of genomic tail DNA (Fig. 1D). CD151-null homozygotes were generated by interbreeding of heterozygotes and were produced in Mendelian ratios.

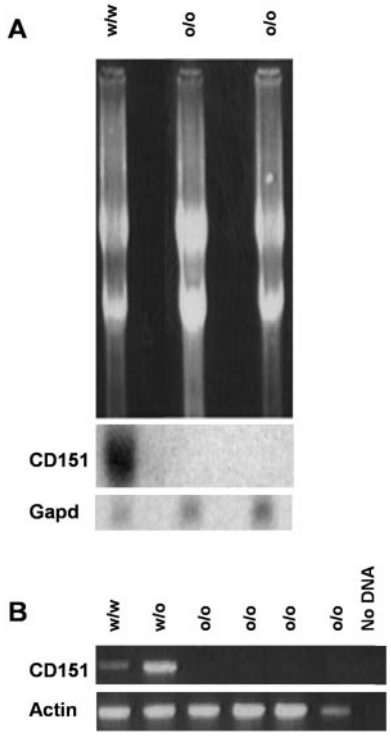

FIG. 2. Confirmation of lack of CD151 mRNA. (A) In the Northern blot analysis, 15 μg of total lung RNA was isolated from wild-type (w/w) and knockout (o/o) mice, separated on an agarose gel (top, ethidium bromide stain), and probed with CD151 cDNA (middle). After stripping, the filter was reprobed with glyceraldehhyde-3-phosphate dehydrogenase (GAPD) cDNA (bottom). (B) Reverse transcriptase-PCR analysis. cDNA was transcribed from lung RNA isolated from wild-type (w/w), heterozygous (w/o), and knockout mice (o/o). CD151 and actin cDNAs were specifically amplified by the PCR.

To confirm that gene targeting and Cre-mediated recombination had successfully inactivated the CD151 gene, Northern blot analysis was performed on mouse lung RNA. Hybridization with a mouse CD151 probe readily detected a 1.8-kb message in wild-type mice. However this message was clearly absent from RNA isolated from CD151-null mice (Fig. 2A). To confirm that the CD151 gene had been inactivated by targeting and Cre-mediated recombination, the more sensitive technique of reverse transcription-PCR was used. Again, while we could readily amplify CD151 cDNA from wild-type and heterozygous mice, CD151 message was consistently undetected in RNA isolated from CD151-null mice (Fig. 2B).

Blood and bone marrow composition. In humans, CD151 is expressed abundantly on megakaryocytes and platelets but at much lower levels by other leukocytes (42). However, both megakaryocyte and platelet numbers and morphology were normal in CD151-null mice (Tables 1 and 2). Relative to wild-type C57BL/6 mice; the null mice showed a slight but signifi-

TABLE 1. Circulating white blood cell counts, megakaryocytes, and differential white blood cell counts for peripheral blood and bone marrow in CD151 knockout mice

Parameter[a]	Value[b] (mean ± SEM)		P[c]
	$CD151^{+/+}$	$CD151^{-/-}$	
WBC count (10^9/liter)	3.76 ± 0.30	3.27 ± 0.36	>0.05
PB neutrophils (%)	5.67 ± 0.82	7.375 ± 1.16	>0.05
PB lymphocytes (%)	93.50 ± 0.94	91.63 ± 1.30	>0.05
PB monocytes (%)	0.76 ± 0.36	0.88 ± 0.34	>0.05
PB neutrophils (10^9/liter)	0.23 ± 0.04	0.24 ± 0.05	>0.05
PB lymphocytes (10^9/liter)	3.50 ± 0.28	3.00 ± 0.34	>0.05
PB monocytes (10^9/liter)	0.019 ± 0.013	0.020 ± 0.009	>0.05
BM megakaryocytes, no./film	24.18 ± 1.07	24.63 ± 1.21	>0.05
BM promyelocytes (%)	8.88 ± 1.54	12.36 ± 1.23	<0.0005
BM myelocytes (%)	8.88 ± 0.96	10.87 ± 0.86	>0.05
BM metamyelocytes (%)	3.59 ± 0.67	7.20 ± 0.98	<0.005
BM neutrophil band forms (%)	13.65 ± 0.91	15.40 ± 1.40	>0.05
BM neutrophils (%)	23.82 ± 3.64	25.31 ± 3.02	>0.05
BM lymphocytes (%)	51.00 ± 3.09	40.80 ± 3.81	<0.05
BM monocytes (%)	1.29 ± 0.36	1.20 ± 0.28	<0.05

[a] WBC, white blood cell; PB, peripheral blood; BM, bone marrow.
[b] Results are expressed as the mean ± standard error of mean for 16 in each group.
[c] P values of <0.05 and <0.0005 (Student's t test) were considered statistically significant.

cant increase in the proportion of immature cells of the myeloid lineage in bone marrow (promyelocytes and metamyelocytes) and a corresponding decrease in the proportion of lymphocytes. The CD151-null mice showed no evidence of overt anemia, but analysis of peripheral blood red cell parameters revealed a slight elevation in packed cell volume and mean cell volume.

Tissue architecture and integrin expression. CD151 forms strong complexes with integrins α3β1, α6β1, and α6β4. These integrins play a crucial role in the architecture and function of skin and kidney epithelia (7, 14, 27, 51). Histological examination of these tissues from CD151-null and wild-type mice revealed no apparent morphological differences (Fig. 3A to D). Integrin α6β4 is a component of hemidesmosomes, as is CD151, at least in human skin. Analysis of skin from CD151-null mice by electron microscopy demonstrated the presence of apparently normal hemidesmosome structures and numbers (Fig. 3E and F). The expression of α3 and α6 integrins in kidney tissues was examined by immunohistochemistry (Fig. 4). Expression of both α3 and α6 integrins could be seen, especially in the glomeruli, in sections from both wild-type and CD151-null mice. The data indicate that CD151 is not required for expression of these integrins.

TABLE 2. Circulating red blood cell and platelet parameters for peripheral blood in CD151 knockout mice

Parameter[a]	Value (mean ± SEM)[b]		P[c]
	$CD151^{+/+}$	$CD151^{-/-}$	
RBC count (10^{12}/liter)	7.74 ± 0.118	7.91 ± 0.119	>0.05
Hb (g/liter)	122.9 ± 1.75	122.63 ± 1.81	>0.05
PCV (liters/liter)	0.39 ± 0.006	0.48 ± 0.031	<0.05
MCV (fl)	51.19 ± 0.400	61.1 ± 3.89	<0.05
MCH (pg)	15.88 ± 0.085	15.63 ± 0.125	>0.05
MCHC (g/liter)	309.88 ± 1.81	268.00 ± 14.08	<0.05
PLT (10^9/liter)	787.2 ± 39.16	776.15 ± 51.27	>0.05

[a] RBC, red blood cell; Hb, hemoglobin; MCV, mean cell volume; MCH, mean cell hemoglobin; MCHC, mean cell hemoglobin concentration; PLT, platelet count.
[b] Results are expressed as the mean ± standard error of the mean for 16 in each group.
[c] $P < 0.05$ (Student's t test) was considered statistically significant.

Expression of integrins and tetraspanins by isolated epidermal keratinocytes. To obtain more quantitative data on expression of integrins that are normally associated with CD151 and of other tetraspanins, keratinocyte populations isolated from neonatal skin were studied by indirect immunofluorescence and flow cytometry. Levels of cell surface α3, α6, β1, and β4 integrin chains were indistinguishable between wild-type and CD151-null cells (Fig. 5). CD9 and CD81, other murine tetraspanins expressed in epithelia for which monoclonal antibodies are available, were also examined. CD9 was strongly positive on epidermal keratinocytes, and its level was significantly lower on CD151-null cells. CD81 was not detected on primary keratinocytes from either wild-type or CD151-null animals, although in both cases expression was induced on cells passaged in vitro (data not shown).

CD151-null keratinocytes fail to migrate in vitro. Keratinocyte migration out of punch biopsies of skin from 3-day-old mice in vitro was used as an assay of migratory ability. Keratinocytes from wild-type mice displayed an extensive halo of cells around the explant after 2 to 6 days of culture, whereas reduced, patchy outgrowth was observed with skin from CD151-null mice (Fig. 6). This result was replicated in four separate experiments (see Fig. 7 for two examples). All of the cells were positive when stained with a mixture of antibodies to cytokeratins 5 and 10, confirming that they were keratinocytes (data not shown).

To assess the contribution of proliferation relative to migration to outgrowth, skin specimens were treated with mitomycin C to prevent DNA replication. While this resulted in reducing the outgrowth of cells from explants of wild-type skin, a considerable halo of cells was still observed, suggesting that both proliferation and migration are important in this assay (Fig. 7). Mitomycin C treatment eliminated outgrowth from CD151-null skin explants, implying that the outgrowth that was observed in the absence of drug was dependent on cell proliferation. The proliferation of isolated CD151-null keratinocytes was indistinguishable from that of wild-type keratinocytes in primary cultures over a period of 6 days (data not shown), and together these data indicate that the reduction in outgrowth from explants resulting from the lack of CD151 reflects altered migratory ability.

CD151-null mice display unstable hemostasis. CD151 is expressed by both platelets and vascular endothelium in humans (42), and monoclonal antibodies to CD151 have platelet agonist activity (1). Therefore, the mice were examined for abnormal hemostasis with an in vivo tail bleeding assay. As shown in Fig. 8, there was a small but significant ($P < 0.05$) difference in the mean tail bleeding times for wild-type and CD151-null mice, and the spread of the data for the CD151-null mice indicated that some CD151-null mice had prolonged bleeding times (Fig. 8A). Consistent with this

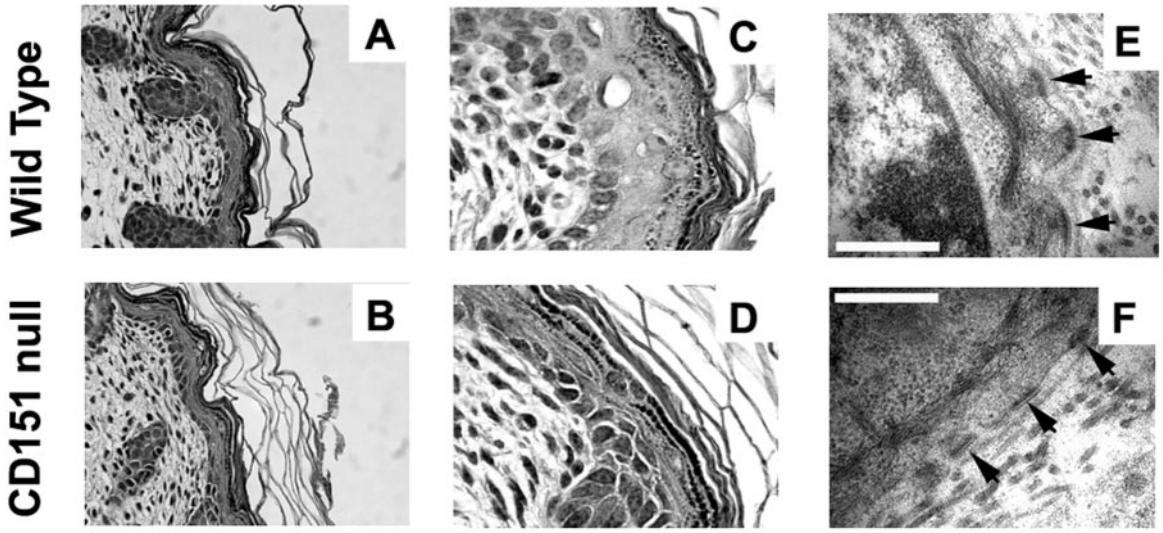

FIG. 3. Skin morphology in wild-type and CD151-null mice. Sections of wild-type (A, C, and E) and CD151-null (B, D, and F) skin were examined by light and electron microscopy. Formaldehyde-fixed sections stained with hematoxylin and eosin were photographed at ×400 (A and B) and ×1,000 (C and D) magnification. Electron microscopy (E and F) was carried out to visualize hemidesmosomes (arrowed). Bars, 500 nm.

feature, the mean volume of blood lost during tail bleeding time was threefold greater for CD151 knockout mice than for wild-type mice (Fig. 8B), and the difference between groups was again significant ($P < 0.05$). The percentage of rebleeds for CD151-null mice was significantly higher (35% compared to 5%; $P < 0.005$) for the wild-type mice, indicating unstable hemostasis (Fig. 8C). Based on this in vivo bleeding defect, the CD151-null mice appear to have underlying functional endothelial and/or platelet defects.

CD151-null T lymphocytes are hyperresponsive to mitogenic stimulation. To study the CD151-deficient immune response, mice were immunized with the classical hapten carrier antigen NP-keyhole limpet hemocyanin, and specific immunoglobulin G1 responses were monitored (Fig. 9A). The antibody responses of the CD151-null mice were indistinguishable from those of the wild-type controls. This result was consistent with the proliferative responses of CD151-null splenocytes to the B-cell-specific mitogen lipopolysaccharide (Fig. 9B), which were again comparable to those of the wild-type controls. However, when stimulated with the T-cell mitogen concanavalin A, CD151-null splenocytes reproducibly showed a two- to threefold enhancement of proliferation. To examine the responses of CD151-null T cells in greater detail, T cells were purified and stimulated by cross-linking with a monoclonal antibody against CD3 and the costimulatory molecule, CD28. Again, CD151-null T cells showed significant hyperproliferation (right panel, Fig. 9C). However, a more striking hyperproliferative effect was observed when T cells were stimulated with CD3 in the absence of costimulatory signals (Fig. 9C, left panel). The hyperproliferative phenotype was observed in both $CD4^+$ and $CD8^+$ T cells (Fig. 9D).

DISCUSSION

CD151-null mice were normal, healthy, and fertile. That CD151-null mice were normal, healthy, and fertile was some-

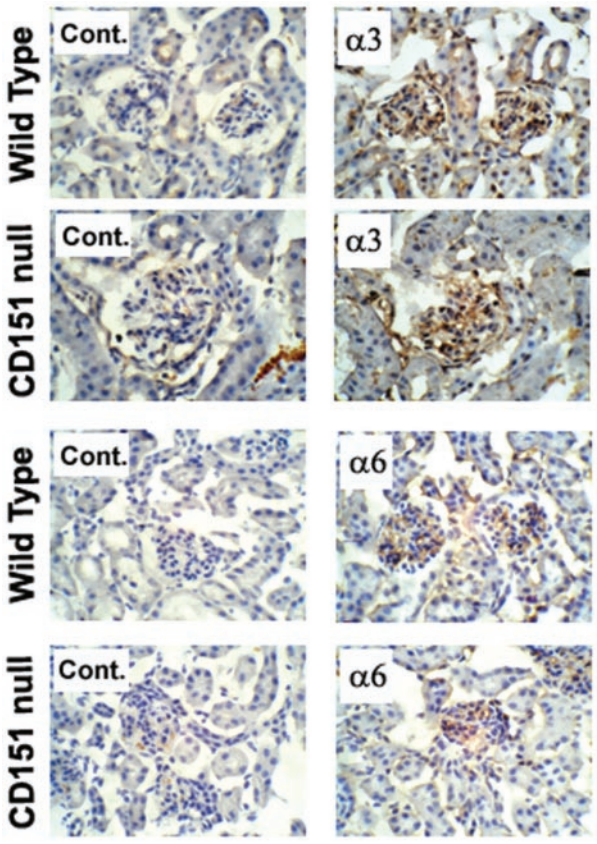

FIG. 4. Normal expression of α3 and α6 integrins in kidneys of CD151-null mice. Kidneys from CD151-null and wild-type mice, 6 to 8 weeks old, were fixed and embedded in OCT, and 5-μm cryostat sections were cut. Sections were stained, as indicated, with polyclonal rabbit antibody to α3 integrin, normal rabbit serum (control for upper panels), rat monoclonal antibody to α6 integrin (GoH3), or normal rat immunoglobulin G (control for lower panels). Magnification, ×400.

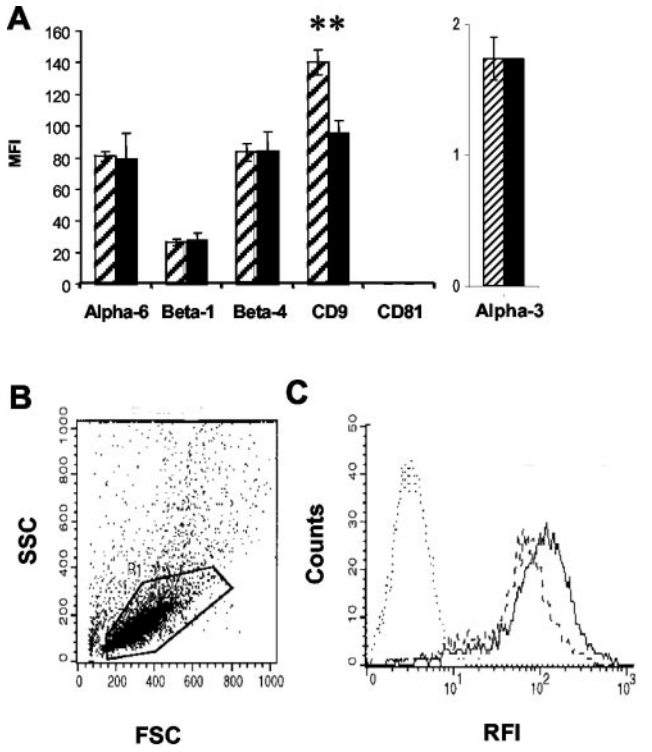

FIG. 5. Quantitation of integrin and tetraspanin expression on isolated keratinocytes. Epidermal keratinocytes isolated from the skins of wild-type and CD151-null neonatal mice (three in each case) were tested for expression of the indicated integrin chains and the tetraspanin CD9 by indirect immunofluorescence and flow cytometry. Since the antibody to α3 detects an intracellular epitope, in that case cells were fixed with formaldehyde and saponin-permeabilized prior to staining. In all other cases, cell surface expression was examined on unfixed cells. (A) Data are shown as the mean and standard error of the mean of the mean fluorescence intensity (MFI) for cells derived from individual mice after subtracting the appropriate negative-control value. Shaded bars indicate wild-type cells, and solid bars indicate CD151-null cells. **, CD9 expression was significantly lower on CD151-null cells ($P < 0.005$, Student's t test). No other significant differences were observed. (B) Typical two-dimensional forward scatter (FSC) plot indicating the gated cell population. (C) Comparison of typical flow cytometry histograms for a wild-type (solid line) and a CD151-null (dashed line) population stained for CD9 expression. The normal rat serum immunoglobulin control is indicated by the dotted line. RFI, relative fluorescence intensity (log scale).

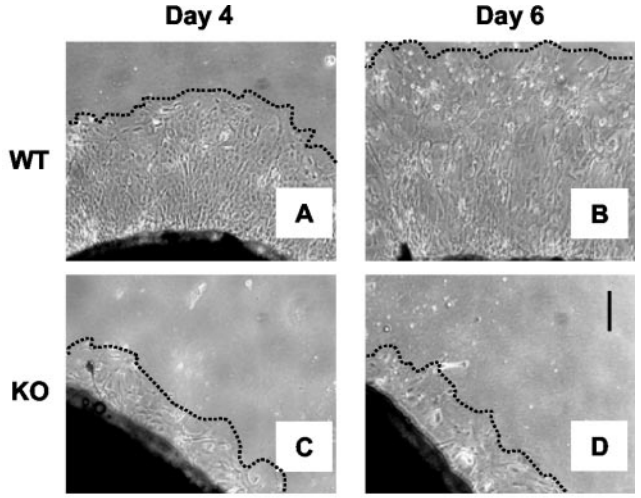

FIG. 6. Keratinocytes from CD151$^{-/-}$ mice display defective outgrowth in skin explant cultures. Skin explants from 2- to 3-day-old wild-type (WT) (A and B) and CD151-null (KO) (C and D) mice were cultured for 6 days, and outgrowth of cells was monitored by microscopy at days 4 (A and C) and 6 (B and D). The same fields were photographed at the two time points. Bar, 200 μm. Dotted lines indicate the extent of the outgrowth.

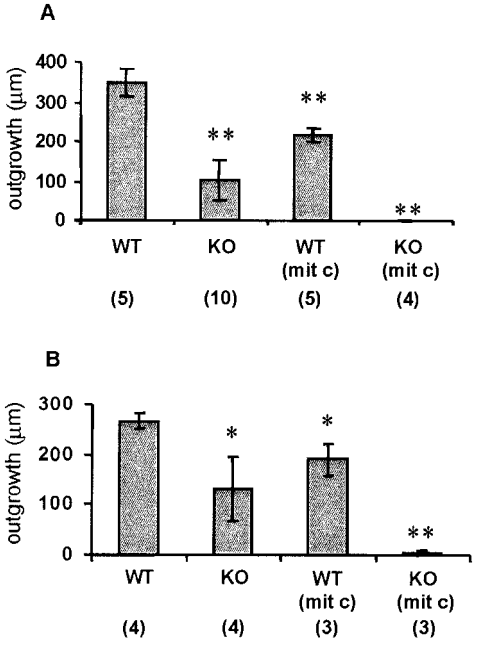

FIG. 7. Residual outgrowth in CD151$^{-/-}$ explant cultures is dependent on cell proliferation. Inhibition of cell proliferation with mitomycin C reduced outgrowth from wild-type (WT) explants and abolished outgrowth from CD151-null (KO) explants. The number of replicates is indicated in parentheses, and error bars indicate the standard error of the mean. (A) Experiment 1. For each explant, the outgrowth was measured on day 4 at eight equally spaced points around the circumference, and the average value was used for analysis. (B) Experiment 2. For each explant, the maximal outgrowth was measured after 2 days of culture. The differences between groups were statistically significant: *, $P < 0.05$; **, $P < 0.005$, relative to the control (wild-type) group (Student's t test).

what surprising because CD151 forms direct associations with the α3 integrin chain that are uniquely strong among tetraspanin-integrin interactions, and it has been hypothesized that CD151 might be required for surface expression of α3β1 (23, 43, 55, 56). Similarly, CD151 forms strong complexes with α6 integrins and mediates α6β1 integrin-dependent cell morphogenesis in vitro (59). Furthermore, in human skin, CD151-α6β4 complexes are a component of hemidesmosomes, which are specialized adhesion structures linking basal keratinocytes to the basement membrane (44). Therefore, we had predicted that the CD151 knockout might result in a phenotype similar to that of mice with deletion of genes encoding α3, α6, or β4 integrins, all of which display neonatal lethality.

In the case of the α3 knockout, lethality was primarily due to defects in kidney and lung development (27). Glomerular de-

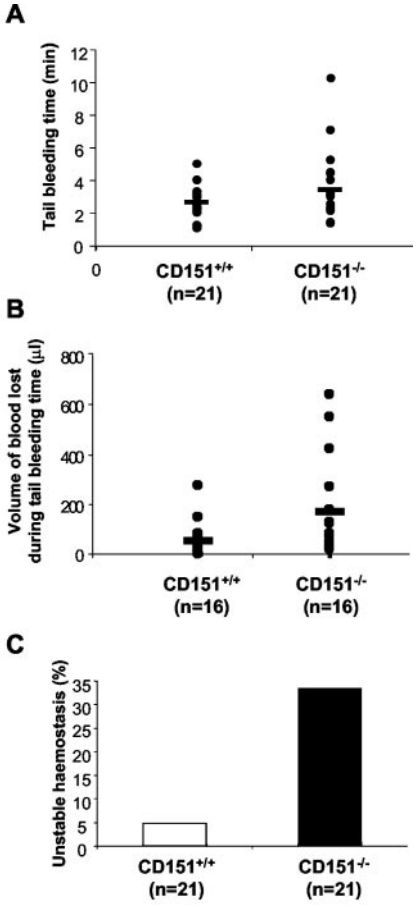

FIG. 8. CD151-null mice have an in vivo bleeding defect. Hemostasis in 6- to 8-week-old mice was assessed with a tail bleeding assay. (A) Time taken for initial cessation of bleeding for wild-type and CD151-null mice. (B) Volume of blood lost during tail bleeding for wild-type and CD151-null mice. Horizontal bars indicate the mean values of the tail bleeding time for each genotype, and each dot represents an individual mouse. (C) Rebleeding occurrences in wild-type and CD151-null mice. In each case the difference between groups was statistically significant: panel A, $P < 0.05$; panel B, $P < 0.05$; panel C, $P < 0.005$ (Student's t test).

velopment was notably markedly abnormal, and the basement membrane was disorganized. In the lungs, branching of the bronchi was decreased (27). Subsequent studies revealed that skin development was also abnormal in α3-null mice, with detachment due to rupture of the basement membrane (7). Knockouts of the α6 and β4 integrin chains have a remarkably similar phenotype, reflecting the crucial role of the α6β4 heterodimer in adhesion of basal keratinocytes to the basement membrane via hemidesmosomes. These mice, like those lacking another hemidesmosome component, BPAG1/BP230, display skin blistering due to detachment of the epidermis from the basement membrane (14, 51).

Although the α6β4 integrin complex (but not hemidesmosomes) is present in other tissues, such as some endothelial cells, thymocytes, and Schwann cells, no abnormalities of these cells were observed in α6- or β4-null mice. Surprisingly, no structural abnormality of the skin or kidney of CD151-null mice was detected at the light microscopy level, and hemides-

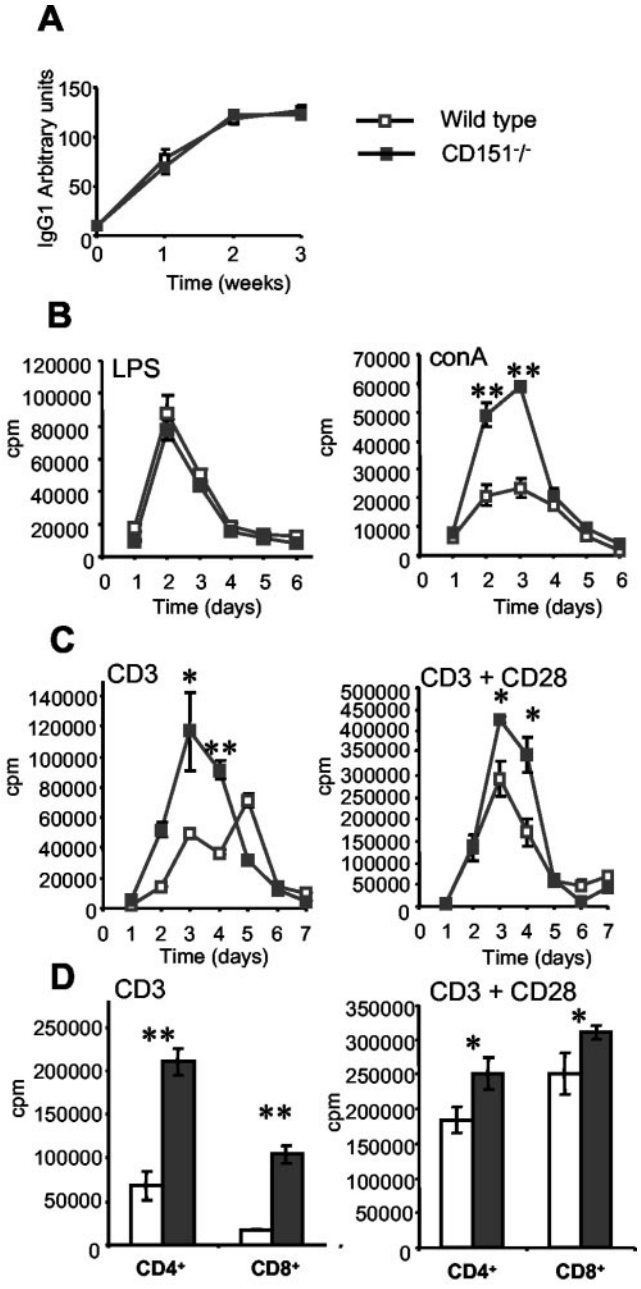

FIG. 9. Immune responses in CD151-null mice. (A) NP-specific immunoglobulin G1 serum antibody responses of wild-type ($n = 8$) and CD151-null ($n = 8$) mice. Data are expressed as arbitrary units calculated from a standard curve. (B) In vitro proliferative responses of splenocytes isolated from wild-type (open squares) and CD151-null (solid squares) mice, stimulated with 1 μg of lipopolysaccharide (left panel) or concanavalin A (right panel) per ml. (C) In vitro proliferative responses of T lymphocytes purified from wild-type (solid squares) and CD151-null (open squares) mice stimulated with 10 μg of anti-CD3 (left panel) or 10 μg of anti-CD3 plus 1 μg of anti-CD28 monoclonal antibody (right panel) per ml. (D) In vitro proliferative responses of $CD4^+$ (day 4) and $CD8^+$ (day 3) T lymphocytes purified from wild-type (open bars) and CD151-null (solid bars) mice stimulated with 10 μg of anti-CD3 monoclonal antibody (left panel) or 10 μg of anti-CD3 plus 1 μg of anti-CD28 monoclonal antibody (right panel) per ml. The differences between groups were statistically significant: *, $P < 0.05$; **, $P < 0.005$, relative to the control (wild-type) group (Student's t test).

mosomes appeared normal by electron microscopy (Fig. 3). Expression of α3 and α6 integrins was indistinguishable from that in controls by immunohistochemistry on kidney sections (Fig. 4) and by quantitative immunofluorescence analysis on isolated keratinocytes (Fig. 5) CD151 also forms strong complexes with the α7β1 integrin (45), and knockout of α7 results in the development of a form of muscular dystrophy soon after birth (32). No evidence of muscle abnormality was seen in CD151-null mice observed for up to 1 year of age. These observations indicate that CD151 is not essential for α3, α6, or α7 integrin expression or function.

A murine tetraspanin sequence very closely related to CD151 has been identified by database mining (19). BAB22942 displays a remarkable 57% identity to mouse CD151 at the protein level; by contrast, the level of identity between CD151 and other typical tetraspanin molecules is on the order of 25%. In general, the transmembrane domains of tetraspanins are highly conserved, whereas the major extracellular domains are relatively divergent. It is therefore remarkable that the extracellular domains of CD151 and BAB22942 also display 57% identity. The region of CD151 that mediates the interaction with α3β1 integrin has been mapped to an 11-amino-acid motif (RDHASNIYKVE) that resides in the large extracellular domain (3). The sequence of the equivalent region in the BAB22942 is very highly conserved (RAHPSNIYKVE) and differs at only 2 of the 11 amino acids. This suggests that BAB22942 might also form tight associations with α3, α6, and α7 integrins, possibly compensating for some functions of CD151. Other tetraspanins, CD9 and CD81, that complex with α3 and α6 integrins are believed to interact indirectly via CD151 (40). Interestingly, cell surface expression of CD9 was significantly reduced on isolated CD151-null keratinocytes compared to wild-type cells when examined by quantitative immunofluorescence and flow cytometry (Fig. 5), possibly reflecting the requirement for CD151 for CD9 incorporation into these integrin complexes (40). CD81 was not expressed on the surface of either wild-type or CD151-null keratinocytes. It is therefore unlikely that either of these tetraspanins compensates for the lack of CD151 in skin.

Although deletion of the CD151 gene did not cause major phenotypic disruption, it seemed likely that more subtle functional effects might be seen in specific tissues. In humans, CD151 is expressed in most tissues (10), notably in cells of the platelet-megakaryocyte lineage and epithelial, endothelial, and muscle cells (42). CD151 expression is abundant in megakaryocytes, and we predicted that it might be required for interaction of these cells with the endothelium in platelet generation. However, both bone marrow megakaryocyte and blood platelet numbers and morphology were normal in the null mice (Tables 1 and 2). Analysis of blood and bone marrow differential cell counts indicated a slight but significant shift towards immature cells in the myeloid lineage. This could arise from altered interactions with bone marrow stromal cells in the null mice, since these stroma normally express CD151 (10).

To look for defects in platelet and/or endothelial cell function, a study of in vivo tail bleeding time was carried out. Although there was only a minor difference in the bleeding time endpoint, the volume of blood lost and the tendency to rebleed were greater in the CD151-null mice (Fig. 8). These results support a moderate in vivo tail bleeding defect, indicating unstable hemostasis. As CD151 is expressed on the surface of platelets and endothelial cells, this abnormality may be attributed to a defect in either platelet-platelet or platelet-endothelium associations. Further detailed studies will be required to resolve this issue.

Tetraspanins have been shown to regulate cell migration, including that of keratinocytes (37). Integrins α3β1 and α6β4, both of which form tight complexes with CD151, play a critical role in this process (12, 15, 16). As a measure of cell motility, we investigated the ability of keratinocytes from wild-type and CD151-null mice to migrate out of punch biopsies of neonatal skin in vitro. CD151-null keratinocytes were clearly defective in their ability to migrate in this assay (Fig. 6). The assay is regarded as a model for wound healing rather than skin development (33). The lack of an obvious skin phenotype in CD151-null mice suggests different regulation of these processes. It will be important to extend the studies of CD151-null mice to assays of in vivo wound healing.

CD151 expression is low on resting lymphocytes but is upregulated on T-cell activation (18). T-cell-dependent antibody responses appeared to be normal in the CD151-deficient immune system; moreover, CD151-null B cells responded normally in vitro to mitogenic stimulation. However, CD151-null T cells were notably hyperproliferative in response to in vitro stimulation, particularly when stimulated through the T-cell receptor in the absence of costimulatory signals. Remarkably, of the five tetraspanin knockouts so far reported, four show an apparently similar hyperproliferative T-cell phenotype: CD81 (36), CD37 (52), TSSC6 (48), and now CD151. Given the propensity of tetraspanins to associate with each other in supramolecular complexes, it seems reasonable to speculate that there is a common regulatory function for tetraspanins in T-cell proliferation.

Thus, although mice lacking CD151 are grossly normal and healthy, we have identified functional abnormalities in all the systems that have been examined in detail in which CD151 has been proposed to play a role. Several additional systems remain to be examined. For example, based on antibody inhibition studies in vitro, CD151 appears to influence angiogenesis (43). A monoclonal antibody to CD151 was reported to block human neutrophil motility in response to the chemotactic peptide formyl-Met-Leu-Phe (55), and it will be important to examine CD151-null mice in models of inflammation. In the nervous system, monoclonal antibody to CD151 inhibited neurite outgrowth in vitro (46), and the protein is abundantly expressed by Schwann cells in the peripheral nervous system (42). CD151 is coexpressed with integrin α7β1 in smooth, cardiac, and skeletal muscle (45), and it may regulate adhesion strengthening to basement membrane laminin in these tissues. Integrin α6β1-dependent adhesion strengthening on Matrigel was enhanced in NIH 3T3 cells overexpressing CD151 (28).

Like CD151, and in contrast to knockouts affecting integrin chains, knockouts of other tetraspanins have so far led to relatively mild phenotypes. Similar to CD151, CD9 and CD81 are widely expressed in tissues and also complex with integrins (2, 40). However, homozygous deletion of CD9 resulted in a highly specific effect on female fertility due to the failure of sperm-egg fusion (22, 29, 35). Deletion of CD81 resulted in defects in B-cell function but increased T-cell proliferation (30, 36). More recently, it was shown that CD81-null mice have "big

brains" because of loss of proliferative arrest of CD81-null astrocytes as a result of contact with neuronal cells (13, 24). The tetraspanin CD37 is not widely expressed, and CD37 knockout mice are viable but display defects in B-cell function, B- and T-cell interaction, and T-cell proliferation (25, 52). The expression of the recently described tetraspanin TSSC6 is restricted to hematopoietic cells; knockout mice are viable, with normal lymphoid development, but, like CD37 and CD81 knockout mice, their T cells are hyperproliferative (48).

The relatively mild phenotypes of mice with knockouts of tetraspanins may be due to complementation of function by other tetraspanins or because tetraspanins function as modifiers rather than essential components of the molecular complexes in which they participate (31). In order to resolve this, studies with combinatorial tetraspanin knockouts and further biochemical experiments will be required.

ACKNOWLEDGMENTS

This work was supported by grants from the National Health and Medical Research Council of Australia (NHMRC) and the National Heart Foundation and by infrastructure funding from NSW Health through the Hunter Medical Research Institute. L.K.A. is an NHMRC Principal Research Fellow and Brawn Professorial Fellow of the University of Newcastle, Australia. D.E.J. is an NHMRC Senior Research Fellow, and V.A. is an NHMRC R. D. Wright Fellow.

We thank Annemiek van Spriel for helpful discussions; Sandra Isenmann, Laleh Khalilazar, Kate Gartlan, and Mariam Sofi for technical assistance; Amanda Harman and Debbie Pepperall, University of Newcastle, for assistance with mouse perfusion and skin histology; and Fedor Berditchevski and Scott Todd for the gift of antibodies. Special thanks go to Rob Parton and Charles Ferguson, Centre for Microscopy and Microanalysis, University of Queensland, Australia, for electron microscopy on skin and to John Bertram, Monash University, Melbourne, for advice on preparation of kidney specimens.

REFERENCES

1. **Ashman, L. K., G. Aylett, P. Mehrabani, L. Bendall, S. Niutta, A. C. Cambareri, S. R. Cole, and M. Berndt.** 1991. The murine monoclonal antibody, 14A2. H1, identified a novel platelet surface antigen. Br. J. Haematol. **79:** 263–270.
2. **Berditchevski, F.** 2001. Complexes of tetraspanins with integrins: more than meets the eye. J. Cell Sci. **114:**4143–4151.
3. **Berditchevski, F., E. Gilbert, M. R. Griffiths, S. Fitter, L. Ashman, and S. J. Jenner.** 2001. Analysis of the CD151-alpha3beta1 integrin and CD151-tetraspanin interactions by mutagenesis. J. Biol. Chem. **276:**41165–41174.
4. **Berditchevski, F., E. Odintsova, S. Sawada, and E. Gilbert.** 2002. Expression of the palmitoylation-deficient CD151 weakens the association of alpha 3 beta 1 integrin with the tetraspanin-enriched microdomains and affects integrin-dependent signaling. J. Biol. Chem. **277:**36991–37000.
5. **Boucheix, C., and E. Rubinstein.** 2001. Tetraspanins. Cell. Mol. Life Sci. **58:**1189–1205.
6. **Chattopadhyay, N., Z. Wang, L. K. Ashman, S. Brady-Kalnay, and J. Kreidberg.** 2003. α3β1 integrin: CD151, a component of the cadherin-catenin complex, regulates PTPu expression and cell-cell adhesion. J. Cell Biol. **163:**1351–1362.
7. **DiPersio, C. M., K. M. Hodivala-Dilke, R. Jaenisch, J. A. Kreidberg, and R. O. Hynes.** 1997. alpha3beta1 Integrin is required for normal development of the epidermal basement membrane. J. Cell Biol. **137:**729–742.
8. **Fitter, S., M. F. Seldin, and L. K. Ashman.** 1998. Characterisation of the mouse homologue of CD151 (PETA-3/SFA-1); genomic structure, chromosomal localisation and identification of 2 novel splice forms. Biochim. Biophys. Acta **1398:**75–85.
9. **Fitter, S., P. Sincock, C. Jolliffe, and L. K. Ashman.** 1999. Transmembrane 4 superfamily protein CD151 (PETA-3) associates with beta 1 and alpha IIb beta 3 integrins in haemopoietic cell lines and modulates cell-cell adhesion. Biochem. J. **338:**61–70.
10. **Fitter, S., T. Tetaz, M. Berndt, and L. K. Ashman.** 1995. Molecular cloning of cDNA encoding a novel platelet-endothelial cell tetra-span antigen, PETA-3. Blood **86:**1348–1355.
11. **Flint, M., C. Maidens, L. Loomis-Price, C. Shotton, J. Dubuisson, P. Monk, A. Higginbottom, S. Levy, and J. McKeating.** 1999. Characterization of hepatitis C virus E2 glycoprotein interaction with a putative cellular receptor, CD81. J. Virol. **73:**6235–6244.
12. **Fuchs, E., J. Dowling, J. Segre, S. H. Lo, and Q. C. Yu.** 1997. Integrators of epidermal growth and differentiation: distinct functions for beta 1 and beta 4 integrins. Curr. Opin. Genet. Dev. **7:**672–682.
13. **Geisert, E. E., Jnr, R. W. Williams, G. R. Geisert, L. Fan, A. M. Asbury, H. T. Maecker, J. Deng, and S. Levy.** 2002. Increased brain size and glial cell number in CD81-null mice. J. Comp. Neurol. **453:**22–32.
14. **Georges-Labouesse, E., N. Messaddeq, G. Yehia, L. Cadalbert, A. Dierich, and M. Le Meur.** 1996. Absence of integrin alpha 6 leads to epidermolysis bullosa and neonatal death in mice. Nat. Genet. **13:**370–373.
15. **Giancotti, F. G., and E. Ruoslahti.** 1999. Integrin signaling. Science **285:** 1028–1032.
16. **Goldfinger, L. E., S. B. Hopkinson, G. W. deHart, S. Collawn, J. R. Couchman, and J. C. Jones.** 1999. The alpha3 laminin subunit, alpha6beta4 and alpha3beta1 integrin coordinately regulate wound healing in cultured epithelial cells and in the skin. J. Cell Sci. **112:**2615–2629.
17. **Hakkinen, L., L. Koivisto, and H. Larjava.** 2002. An improved method for culture of epidermal keratinocytes from mouse skin. Methods Cell Sci. **23:**189–196.
18. **Hasegawa, H., Y. Utsunomiya, K. Kishimoto, K. Yanagisawa, and S. Fujita.** 1996. SFA-1, a novel cellular gene induced by human T-cell leukemia virus type 1, is a member of the transmembrane-4 superfamily. J. Virol. **70:**3258–3263.
19. **Hemler, M. E.** 2001. Specific tetraspanin functions. J. Cell Biol. **155:**1103–1107.
20. **Hynes, R.** 2002. Integrins: bidirectional, allosteric signaling machines. Cell **110:**673–687.
21. **Iwamoto, R., S. Higashiyama, T. Mitamura, M. Taniguchi, M. Klagsbrun, and E. Mekada.** 1994. Heparin-binding EGF-like growth factor, which acts as the diphtheria toxin receptor, forms a complex with membrane protein DRAP27/CD9, which up-regulates functional receptors and diphtheria toxin sensitivity. EMBO J. **13:**2322–2330.
22. **Kaji, K., S. Oda, T. Shikano, T. Ohnuki, Y. Uematsu, J. Sakagami, N. Tada, S. Miyazaki, and A. Kudo.** 2000. The gamete fusion process is defective in eggs of Cd9-deficient mice. Nat. Genet. **24:**279–282.
23. **Kazarov, A. R., X. Yang, C. S. Stipp, B. Sehgal, and M. E. Hemler.** 2002. An extracellular site on tetraspanin CD151 determines alpha 3 and alpha 6 integrin-dependent cellular morphology. J. Cell Biol. **158:**1299–1309.
24. **Kelic, S., S. Levy, C. Suarez, and D. E. Weinstein.** 2001. CD81 regulates neuron-induced astrocyte cell-cycle exit. Mol. Cell. Neurosci. **17:**551–560.
25. **Knobeloch, K. P., M. D. Wright, A. F. Ochsenbein, O. Liesenfeld, J. Lohler, R. M. Zinkernagel, I. Horak, and Z. Orinska.** 2000. Targeted inactivation of the tetraspanin CD37 impairs T-cell-dependent B-cell response under suboptimal costimulatory conditions. Mol. Biol. Cell **20:**5363–5369.
26. **Kontgen, F., G. Suss, C. Stewart, M. Steinmetz, and H. Bluethmann.** 1993. Targeted disruption of the MHC class II Aa gene in C57BL/6 mice. Int. Immunol. **5:**957–964.
27. **Kreidberg, J. A., M. J. Donovan, S. L. Goldstein, H. Rennke, K. Shepherd, R. C. Jones, and R. Jaenisch.** 1996. Alpha 3 beta 1 integrin has a crucial role in kidney and lung organogenesis. Development **122:**3537–3547.
28. **Lammerding, J., A. R. Kazarov, H. Huang, R. T. Lee, and M. E. Hemler.** 2003. Tetraspanin CD151 regulates alpha6beta1 integrin adhesion strengthening. Proc. Natl. Acad. Sci. USA **100:**7616–7621.
29. **Le Naour, F., E. Rubinstein, C. Jasmin, M. Prenant, and C. Boucheix.** 2000. Severely reduced female fertility in CD9-deficient mice. Science **287:**319–321.
30. **Maecker, H. T., and S. Levy.** 1997. Normal lymphocyte development but delayed humoral immune response in CD81-null mice. J. Exp. Med. **185:** 1505–1510.
31. **Maecker, H. T., S. C. Todd, and S. Levy.** 1997. The tetraspanin superfamily: molecular facilitators. FASEB J. **11:**428–442.
32. **Mayer, U., G. Saher, R. Fassler, A. Bornemann, F. Echtermeyer, H. von der Mark, N. Miosge, E. Poschl, and K. von der Mark.** 1997. Absence of integrin alpha 7 causes a novel form of muscular dystrophy. Nat. Genet. **17:**318–323.
33. **Mazzalupo, S., M. J. Wawersik, and P. A. Coulombe.** 2002. An ex vivo assay to assess the potential of skin keratinocytes for wound epithelialization. J. Investig. Dermatol. **118:**866–870.
34. **Mittelbrunn, M., M. Yanez-Mo, D. Sancho, A. Ursa, and F. Sanchez-Madrid.** 2002. Cutting edge: dynamic redistribution of tetraspanin CD81 at the central zone of the immune synapse in both T lymphocytes and APC. J. Immunol. **169:**6691–6695.
35. **Miyado, K., G. Yamada, S. Yamada, H. Hasuwa, Y. Nakamura, F. Ryu, K. Suzuki, K. Kosai, K. Inoue, A. Ogura, M. Okabe, and E. Mekada.** 2000. Requirement of CD9 on the egg plasma membrane for fertilization. Science **287:**321–324.
36. **Miyazaki, T., U. Muller, and K. S. Campbell.** 1997. Normal development but differentially altered proliferative responses of lymphocytes in mice lacking CD81. EMBO J. **16:**4217–4225.
37. **Penas, P. F., A. Garcia-Diez, F. Sanchez-Madrid, and M. Yanez-Mo.** 2000. Tetraspanins are localized at motility-related structures and involved in normal human keratinocyte wound healing migration. J. Investig. Dermatol. **114:**1126–1135.
38. **Sawada, S., M. Yoshimoto, E. Odintsova, N. A. Hotchin, and F. Berditchev-**

ski. 2003. The tetraspanin CD151 functions as a negative regulator in the adhesion-dependent activation of Ras. J. Biol. Chem. **278:**26323–26326.
39. **Schwenk, F., U. Baron, and K. Rajewsky.** 1995. A cre-transgenic mouse strain for the ubiquitous deletion of loxP-flanked gene segments including deletion in germ cells. Nucleic Acids Res. **23:**5080–5081.
40. **Serru, V., F. Le Naour, M. Billard, D. Azorsa, F. Lanza, C. Boucheix, and E. Rubinstein.** 1999. Selective tetraspan-integrin complexes (CD81/alpha4beta1, CD151/alpha3beta1, CD151/alpha6beta1) under conditions disrupting tetraspan interactions. Biochem. J. **340:**103–111.
41. **Silvie, O., E. Rubinstein, J. Franetich, M. Prenant, E. Belnoue, L. Renia, L. Hannoun, W. Eling, S. Levy, C. Boucheix, and D. Mazier.** 2003. Hepatocyte CD81 is required for Plasmodium falciparum and Plasmodium yoelii sporozoite infectivity. Nat. Med. **9:**93–96.
42. **Sincock, P., G. Mayrhofer, and L. K. Ashman.** 1997. Localization of the transmembrane 4 superfamily (TM4SF) member PETA-3 (CD151) in normal human tissues: comparison with CD9, CD63, and alpha5beta1 integrin. J. Histochem. Cytochem. **45:**515–525.
43. **Sincock, P. M., S. Fitter, R. G. Parton, M. C. Berndt, J. R. Gamble, and L. K. Ashman.** 1999. PETA-3/CD151, a member of the transmembrane 4 superfamily, is localised to the plasma membrane and endocytic system of endothelial cells, associates with multiple integrins and modulates cell function. J. Cell Sci. **112:**833–844.
44. **Sterk, L., C. Geuijen, L. Oomen, J. Calafat, H. Janssen, and A. Sonnenberg.** 2000. The tetraspan molecule CD151, a novel constituent of hemidesmosomes, associates with the integrin alha6beta4 and may regulate the spatial organization of hemidesmosomes. J. Cell Biol. **149:**969–982.
45. **Sterk, L. M., C. A. Geuijen, J. G. van den Berg, N. Claessen, J. J. Weening, and A. Sonnenberg.** 2002. Association of the tetraspanin CD151 with the laminin-binding integrins alpha3beta1, alpha6beta1, alpha6beta4 and alpha7beta1 in cells in culture and in vivo. J. Cell Sci. **115:**1161–1173.
46. **Stipp, C. S., and M. E. Hemler.** 2000. Transmembrane-4-superfamily proteins CD151 and CD81 associate with alpha 3 beta 1 integrin, and selectively contribute to alpha 3 beta 1-dependent neurite outgrowth. J. Cell Sci. **113:**1871–1882.
47. **Tarrant, J., L. Robb, A. van Spriel, and M. Wright.** 2003. Tetraspanins: molecular organisers of the leukocyte surface. Trends Immunol. **24:**610–617.
48. **Tarrant, J. M., J. Groom, D. Metcalf, R. Li, B. Borobokas, M. D. Wright, D. Tarlinton, and L. Robb.** 2002. The absence of Tssc6, a member of the tetraspanin superfamily, does not affect lymphoid development but enhances in vitro T-cell proliferative responses. Mol. Cell. Biol. **22:**5006–5018.
49. **Tokuhara, T., H. Hasegawa, N. Hattori, H. Ishida, T. Taki, I. Tachibana, S. Sasaki, and M. Miyake.** 2001. Clinical significance of CD151 gene expression in non-small cell lung cancer. Clin. Cancer Res. **7:**4109–4114.
50. **Travis, G., M. Brennan, P. Danielson, C. Kozak, and J. Sutcliffe.** 1989. Identification of a photoreceptor-specific mRNA encoded by the gene responsible for retinal degeneration slow (rds). Nature **338:**70–73.
51. **van der Neut, R., P. Krimpenfort, J. Calafat, C. M. Niessen, and A. Sonnenberg.** 1996. Epithelial detachment due to absence of hemidesmosomes in integrin beta 4 null mice. Nat. Genet. **13:**366–369.
52. **van Spriel, A. B., K. L. Puls, M. Sofi, P. D., H. Hochrein, Z. Orinska, K. P. Knobeloch, M. Plebanski, and M. D. Wright.** 2003. A regulatory role for CD37 in T cell proliferation. J. Immunol. **172:**2953–2961.
53. **Yanez-Mo, M., A. Alfranca, C. Cabanas, M. Marazuela, R. Tejedor, M. Ursa, L. K. Ashman, M. de Landazuri, and F. Sanchez-Madrid.** 1998. Regulation of endothelial cell motility by complexes of tetraspan molecules CD81/TAPA-1 and CD151/PETA-3 with alpha3 beta1 integrin localized at endothelial lateral junctions. J. Cell Biol. **141:**791–804.
54. **Yanez-Mo, M., M. Mittelbrunn, and F. Sanchez-Madrid.** 2001. Tetraspanins and intercellular interactions. Microcirculation **8:**153–168.
55. **Yauch, R. L., F. Berditchevski, M. B. Harler, J. Reichner, and M. E. Hemler.** 1998. Highly stoichiometric, stable, and specific association of integrin alpha3beta1 with CD151 provides a major link to phosphatidylinositol 4-kinase, and may regulate cell migration. Mol. Biol. Cell **9:**2751–2765.
56. **Yauch, R. L., A. R. Kazarov, B. Desai, R. Lee, and M. E. Hemler.** 2000. Direct extracellular contact between integrin alpha(3)beta(1) and TM4SF protein CD151. J. Biol. Chem. **275:**9230–9238.
57. **Zemni, R., T. Bienvenu, M. Vinet, A. Sefiani, A. Carrie, P. Billuart, N. McDonell, P. Couvert, F. Francis, P. Chafey, F. Fauchereau, G. Friocourt, V. des Portes, A. Cardona, S. Frints, A. Meindl, O. Brandau, N. Ronce, C. Moraine, H. van Bokhoven, H. Ropers, R. Sudbrak, A. Kahn, J. Fryns, C. Beldjord, and J. Chelly.** 2000. A new gene involved in X-linked mental retardation identified by analysis of an X;2 balanced translocation. Nat. Genet. **24:**167–170.
58. **Zhang, X. A., A. L. Bontrager, and M. E. Hemler.** 2001. Transmembrane-4 superfamily proteins associate with activated protein kinase C (PKC) and link PKC to specific beta(1) integrins. J. Biol. Chem. **276:**25005–25013.
59. **Zhang, X. A., A. R. Kazarov, X. Yang, A. L. Bontrager, C. S. Stipp, and M. E. Hemler.** 2002. Function of the tetraspanin CD151-alpha6beta1 integrin complex during cellular morphogenesis. Mol. Biol. Cell **13:**1–11.